Carbohydrate Polymers 97 (2013) 743–752

Contents lists available at SciVerse ScienceDirect

Carbohydrate Polymers

journal homepage: www.elsevier.com/locate/carbpol

Synthesis and characterization of ion-imprinted resin based on carboxymethyl cellulose for selective removal of UO_2^{2+}

M. Monier*, D.A. Abdel-Latif

Chemistry Department, Faculty of Science, Mansoura University, Mansoura, Egypt

ARTICLE INFO

Article history:
Received 17 April 2013
Received in revised form 16 May 2013
Accepted 24 May 2013
Available online xxx

Keywords:
Carboxymethyl cellulose
Grafting
Acrylonitrile
Salicylaldehyde
Molecular imprinting

ABSTRACT

In this work, the surface ion-imprinting technique was employed for the preparation of surface ion-imprinted chelating microspheres resin based on modified salicylaldehyde-carboxymethyl cellulose (U-CMC-SAL) in presence of uranyl ions as a template and formaldehyde as a cross-linker. Various instrumental techniques such as elemental analysis, scanning electron microscope (SEM), FTIR and X-ray diffraction spectra were utilized for full characterization of the prepared polymeric samples. The prepared resin exhibited a higher capability for selective removal of UO_2^{2+} when compared to the non-imprinted resin (N-CMC-SAL). Also, different important parameters such as pH, temperature, time and initial metal ion concentration were examined in order to evaluate the optimum condition for the adsorption process. The results indicated that pH 5 was the best for the UO_2^{2+} uptake, in addition, the adsorption was exothermic in nature, follows the second-order kinetics and the adsorption isotherm showed the best fit with Langmuir isotherm model with maximum adsorption capacity of 180 ± 1 and 97 ± 1 mg/g for both U-CMC-SAL and N-CMC-SAL respectively. Desorption and regeneration were carried out using 0.5 M HNO_3 solution and the results confirmed that the resin keeps about 92% of its original efficiency after five consecutive adsorption–desorption operations.

© 2013 Elsevier Ltd. All rights reserved.

1. Introduction

The technology of molecular imprinting is broadly utilized in fabrication of sensible materials in which selective recognition binding active sites are manufactured to adapt with the dimensions, configuration or functionality of a particular imprint template target specie (Qin, He, Zhang, Li, & Zhang, 2009; Zhou et al., 2013). Molecularly imprinted polymers (MIPs) have extensively been used in various biomedical, pharmaceutical, environmental and industrial applications such as solid phase extraction (Sambe, Hoshina, & Haginaka, 2007; Zhu, Yang, Su, Cai, & Gao, 2005) sensors (Aghaei, Hosseini, & Najafi, 2010; Sergeyeva et al., 2010) catalysis (Pasetto, Maddock, & Resmini, 2005) and controlled drug delivery systems (Suedee et al., 2008, 2010). Various conventional polymerization techniques have been utilized in preparation of MIPs including bulk, suspension and emulsion polymerization (Andersson, 1996; Mayes & Mosbach, 1996; Perez, Whitcombe, & Vulfson, 2000) in addition to the multistep swelling polymerization (Haginaka, 2009) and precipitation polymerization (Ye, Cormack, & Mosbach, 1999). However, these common polymerization techniques may causes some serious disadvantages such as the imperfect removal of the imprinted template molecules from the highly cross-linked deeply embedded recognition sites which will subsequently lower the affinity and capacity of the imprinted polymer toward the template target molecules, in addition to the heterogeneous irregular distribution of the binding sits which is a common problem in bulk polymerization (Ozcan & Sahin, 2007; Yin, Meng, Zhu, Song, & Wang, 2011; Jiang et al., 2009).

In the past few years, the new surface imprinting technique was developed and provided promising results in avoiding the most common drawbacks observed in the ordinary traditional imprinting methods (Monier & Abdel-Latif, 2013b). In surface imprinting, the recognition binding sites are created on the surface of inorganic material supports such as silica and graphene (Yao & Zhou, 2009; Xu, Xu, Zhang, Pan, & Yan, 2010) or organic polymeric supports such as poly(ethylene terephthalate) and polypropylene fibers (Monier & Abdel-Latif, 2013b; Xu, Chen, & Wu, 2012) and the finally resulted adsorbent keeps the shape and physical properties of the used material support.

Carboxymethyl cellulose (CMC), one of the most common derivatives of cellulose and because of its significant properties, *i.e.* water solubility, biocompatibility and lake of toxicity, it was implemented in broad range of industrial applications in several fields such as cosmetics, pharmaceuticals and adhesives (Liu & Berg, 2002; Bajpai & Giri, 2003; Mocanu, Mihai, LeCerf, Picton, & Muller,

* Corresponding author at: Chemistry Department, Faculty of Science, Mansoura University, Mansoura, Egypt, 35516. Tel.: +201003975988.
E-mail address: monierchem@yahoo.com (M. Monier).

0144-8617/$ – see front matter © 2013 Elsevier Ltd. All rights reserved.
http://dx.doi.org/10.1016/j.carbpol.2013.05.062

2004). Among various techniques that are commonly used for cellulosic derivatives modification, free radical graft copolymerization of vinyl monomers has attracted the interest of many researchers (Abdel-Halim & Al-Deya, 2012). Considerable number of researches concerning the graft co-polymerization of vinyl monomers such as N-vinyl formamide (Tripathy, Mishra, & Behari, 2009), vinyl sulfonic acid (Sand, Yadav, & Behari, 2010) and acrylamide (Mohy Eldin, El-Sherif, Soliman, Elzatahry, & Omer, 2011) onto CMC in the recent years.

In the present study, UO_2^{2+} surface ion-imprinted microspheres based on CMC (U-CMC-SAL) were prepared through graft copolymerization of polyacrylonitrile (PAN) onto ionically cross-linked CMC microspheres followed by functionalization with hydrazine and then salicylaldehyde. The resulted chelating microspheres were then loaded with UO_2^{2+} and surface imprinting was carried out by cross-linking the salicylaldehyde moieties using formaldehyde cross-linker. Various instrumental techniques such as FTIR, scanning electron microscope (SEM) and X-ray diffraction spectra were used for sample characterization. The potential of the prepared microspheres for the selective removal of UO_2^{2+} was evaluated by investigating the various parameters influencing the uptake behavior such as pH, initial concentration of the UO_2^{2+} ions, shaking time, and temperature. The adsorption kinetics and thermodynamic parameters of the uptake process were also evaluated.

2. Experimental

2.1. Materials

Sodium salt of carboxymethyl cellulose (CMC) with average viscosity of 400–800 cps (2% aqueous solution at 25 °C) was purchased from Fluka. Acrylonitrile (AN) was supplied by Sigma–Aldrich and purified by 3% aqueous NaOH solution then washed with distilled water until alkali free and stored over anhydrous $CaCl_2$ and molecular sieves. Potassium persulfate (KPS); Thiourea (TU); hydrazine hydrate; salicylaldehyde (SAL), formaldehyde and uranyl nitrate hexahydrate $UO_2(NO_3)_2{\cdot}6H_2O$ were purchased from Sigma–Aldrich and used as received.

2.2. Preparation of CMC cross-linked microspheres

Water/oil (W/O) emulsion technique was utilized in the preparation of the ionically cross-linked CMC microspheres, 5 g of the sodium salt of CMC was dissolved in 100 mL distilled water. After complete dissolution, the W/O emulsion was prepared with ratio 4:17 (v/v) by adding the aqueous CMC solution dropwise to the dispersion medium which contain a mixture of cyclohexane and n-hexanol (11:6) in addition to 1.5 mL Triton X-100 as an emulsifier. During the addition, the dispersion medium was mechanically stirred at about 1000 rpm at room temperature. After 15 min, 20 mL of 50% (w/v) $AlCl_3$ cross-linker solution was added and stirring was continued for 1 h, then an additional 10 mL of the $AlCl_3$ solution was added and the stirring was continued for 15 min. Finally the resulted cross-linked CMC microspheres was separated, washed with distilled water and then by ethanol and finally dried at 50 °C in an oven for 24 h and then stored in a vacuum dessicator for further use.

2.3. Graft copolymerization of PAN onto CMC microspheres

The free radical graft copolymerization of PAN onto the ionically cross-linked CMC microspheres was performed using KPS/TU combined redox initiator according to the following procedures: 1 g of the previously prepared CMC microspheres was dipped in 20 mL of the redox initiator system which composed of 4 mM KPS, 2 mM TU and one drop of 1% sulfuric acid. The mixture was shacked vigorously for 5 min and then 0.15 mol of the acrylonitrile (AN) monomer was added and the reaction was continued for 2 h with stirring at 60 °C. After the completion of the reaction the termination was carried out by addition of 10 mL 3% (w/v) hydroquinone solution. Finally, the resulted products were filtered and washed with DMF to extract the PAN homopolymer. The grafted CMC microspheres were then dried in an oven at 40 °C for 24 h. The grafting percentage (*GP*) was evaluated according to the following equation:

$$\text{Grafting percentage}\quad (GP) = \left(\frac{A-B}{B}\right) \times 100$$

where *A* and *B* are the weight of grafted and native CMC microspheres resin, respectively.

These grafted CMC microspheres prepared with GP values 145% were named as CMC-g-PAN.

2.4. Preparation of (U-CMC-SAL) ion-imprinted microspheres

The following consecutive steps were employed for the surface ion imprinting process:

The previously prepared CMC-g-PAN microspheres were firstly modified by conversion the —CN groups of the grafted PAN chains into the active hydrazidine groups (HN=C—NH—NH_2) through refluxing the microspheres with 100 mL 10% (v/v) alcoholic hydrazine hydrate solution for 2 h at 80 °C. The resulted modified microspheres named as CMC-g-PAH.

In the next step, the previously modified CMC-g-PAH was treated with 100 mL 10% (v/v) alcoholic salicylaldehyde solution and the mixture was refluxed for 4 h at 80 °C. The resulted chelating microspheres named as CMC-SAL. Schematic presentation for the synthetic steps of the CMC-SAL is shown in Scheme 1.

The loading of the UO_2^{2+} ions was performed by immersing 1 g of the prepared CMC-SAL chelating microspheres resin into 200 mL UO_2^{2+} solution (100 mg/L) at pH 5. The content of the mixture was equilibrated on the shaker at 150 rpm and 30 °C for 3 h. The uranyl loaded chelating microspheres were then removed and washed with distilled water to remove the non-adsorbed uranyl ions. The surface ion-imprinting process was then carried out by dipping the uranyl loaded microspheres into 100 mL 35% formaldehyde solution, after raising the pH to 9 by adding the appropriate required amount of NaOH solution, and refluxing the mixture at 80 °C for 8 h. After the completion of the reaction, the template UO_2^{2+} was removed from the cross-linked network using 0.5 M HNO_3 and the process repeated three times to assure the complete removal of template UO_2^{2+} ions. Then, the microspheres resin was removed and washed with ethanol and deionized water and dried at 40 °C. As a control, another sample of the non-imprinted chelating microspheres (N-CMC-SAL) was prepared and treated in the same manner in absence of the template UO_2^{2+}. Schematic presentation for the imprinting process is shown in Scheme 2.

2.5. Characterization of samples

A qualitative simple test was performed in order to confirm the insertion of the salicylaldehyde onto the grafted chains by treatment of the resin microspheres with $FeCl_3$ solution in a test tube to produce a deep violet color.

The elemental analysis (E.A.) of pure CMC, Al-cross-linked CMC microspheres, CMC-g-PAN, CMC-g-PAH, CMC-SAL and U-CMC-SAL was obtained from a Perkin-Elmer 240C Elemental Analytical Instrument (USA).

A Perkin-Elmer Fourier transform infrared spectrometer (FTIR) was utilized to investigate the chemical structure and elucidate the

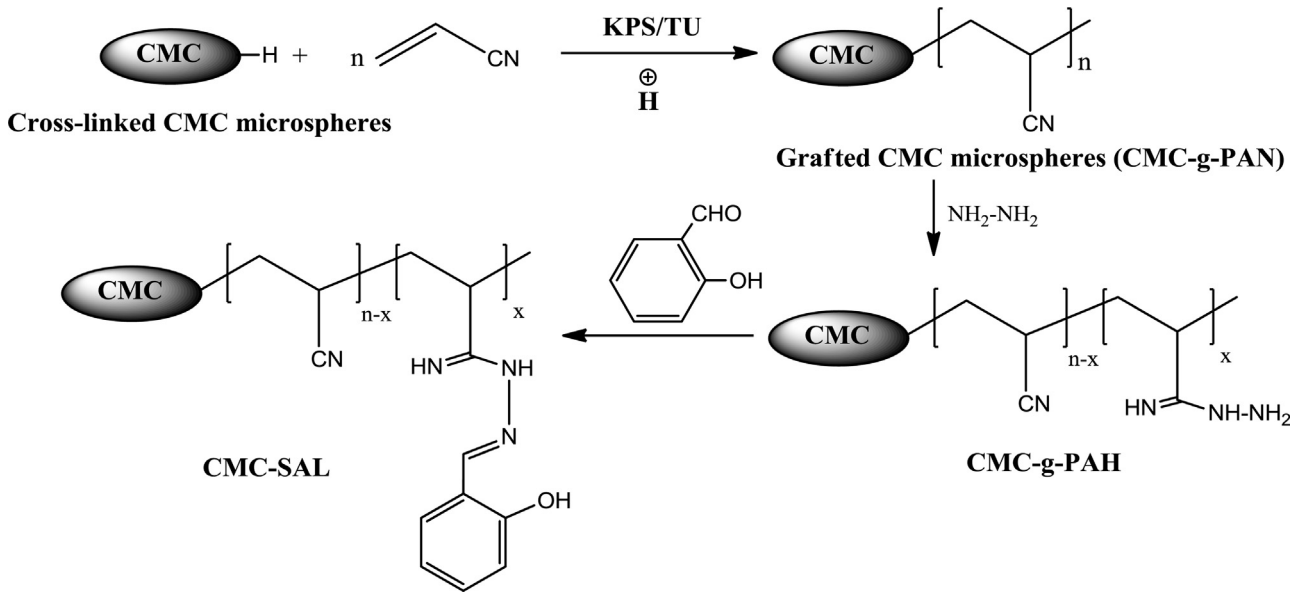

Scheme 1. Synthesis of CMC-SAL chelating microspheres.

modification steps of the polymeric samples. The studied samples were mixed with KBr and compressed in form of discs.

FEI Quanta-200 scanning electron microscope (SEM) (FEI Company, USA) was applied to investigate the changes in the surface morphologies of the synthesized polymeric microspheres upon chemical modifications. The samples were coated with gold for 40 s at 15 mA and 20 kV accelerating voltage.

ASAP 2010 Micromeritics instrument was applied to estimate the surface area of the samples using Brunauer–Emmett–Teller (BET) method and Micromeritics software.

The crystallinity of CMC samples before and after grafting and modification were examined by XRD analysis using X-ray powder diffractometer (Japanese Dmax-rA, wavelength = 1.54 Å, Cu Kα radiation). The samples were scanned from $2\theta = 5–70^{\circ}$, in step of

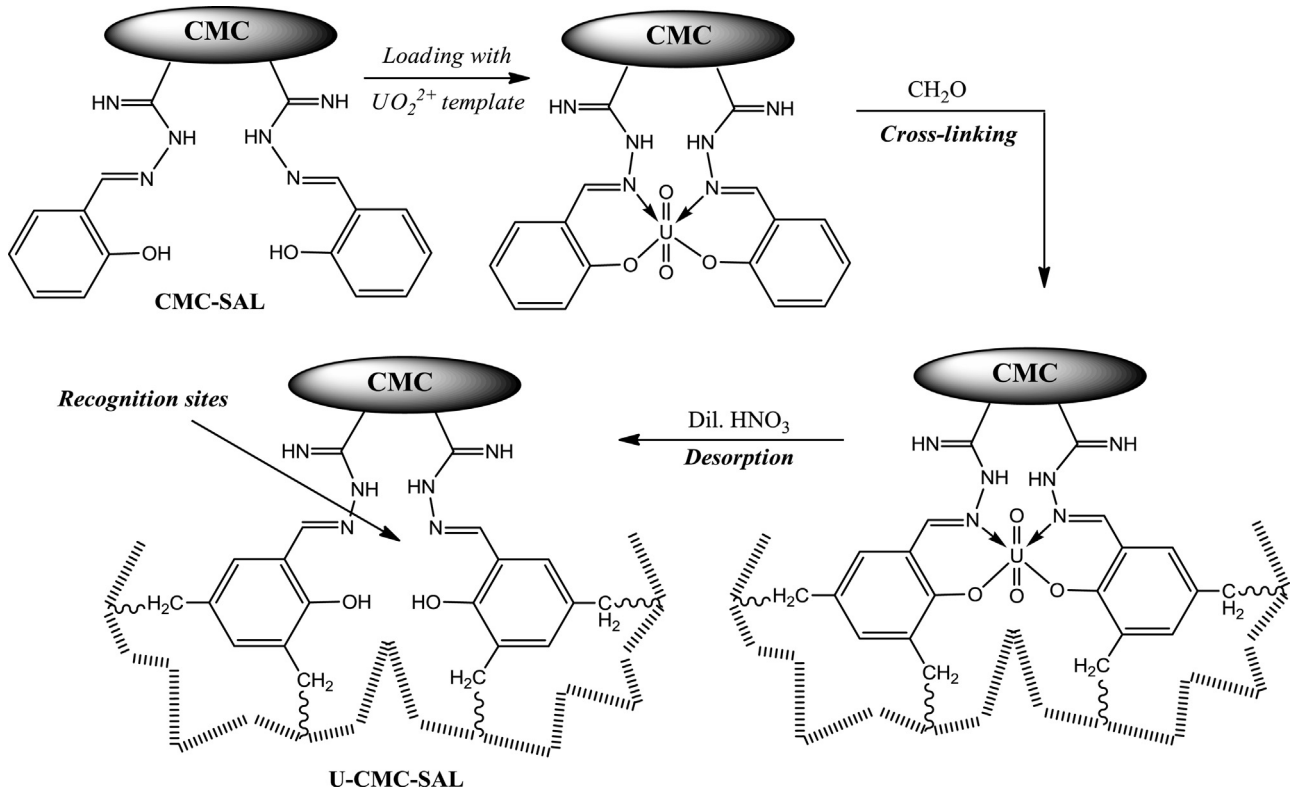

Scheme 2. Ion-imprinting of UO_2^{2+} ions onto CMC-SAL microspheres resin.

0.02° using generator intensity of 40 kV and generator current of 50 mA.

2.6. Adsorption experiments

2.6.1. Effect of pH

For anticipation of the influence of pH, the performance of the adsorption experiments were carried out in a range of pH from 1 to 5 at 30 °C by placing 0.03 g of the dry *U-CMC-SAL* or *N-CMC-SAL* resin in 30 mL metal ion solution with concentration 100 mg/L. The mixture was allowed to equilibrate at 150 rpm for 3 h. The adaptation of the pH was performed using HNO_3/KNO_3 for pH values 1, 2 and 3 and acetic acid/sodium acetate for pH values 4 and 5. Once the adsorption had been accomplished, the Arsenazo I method was utilized to determine the residual content of the UO_2^{2+} using Shimadzu UV-1601 spectrophotometer where the absorbance was measured at 596 nm.

2.6.2. Effect of the temperature

The thermodynamic parameters were anticipated by placing 0.03 g of the dry *U-CMC-SAL* or *N-CMC-SAL* microspheres in 30 mL UO_2^{2+} solution with concentration 30 mg/L. The contents were equilibrated by shacking at 150 rpm at pH 5 for 3 h in a range of temperature changed from 20 to 40 °C and then, the residual UO_2^{2+} concentration was estimated.

2.6.3. Effect of contact time

For estimation of the kinetic parameters, the adsorption experiments were performed by equilibrating 0.3 g of the dry *U-CMC-SAL* or *N-CMC-SAL* microspheres in 300 mL UO_2^{2+} solution with concentration 100 mg/L at pH 5 and 150 rpm at 30 °C. Each 10 min. 1 mL of the metal ion solution was withdrawn for estimation of the residual UO_2^{2+} concentration.

2.6.4. Effect of the initial metal ion concentration

The adsorption isotherm studies were performed by carrying out the UO_2^{2+} uptake experiments in a system containing 0.03 g of both *U-CMC-SAL* and *N-CMC-SAL* microspheres resin in 30 mL of the UO_2^{2+} solution with various concentrations from 10 to 400 mg/L at pH 5.0 and 30 °C for 3 h and 150 rpm.

In all of the previous experiments, the amount of the adsorbed UO_2^{2+} was estimated using the following equations (Monier & Abdel-Latif, 2013a, 2013b).

$$q_e = \frac{(C_i - C_e)V}{W} \tag{2}$$

where q_e (mg/g) is the amount of the adsorbed UO_2^{2+} at equilibrium; C_i (mg/L) and C_e (mg/L) are the initial metal ion concentration and metal ion concentration at equilibrium, respectively, V (L) volume of added solution and W (g) the weight of the used microspheres resin (dry).

$$\text{Percent removal}\ \ (\%) = \frac{(C_i - C_e) \times 100}{C_i} \tag{3}$$

2.6.5. Selective adsorption

For evaluation of the selectivity of the prepared surface ion imprinted microspheres resin, the adsorption of the UO_2^{2+} ions was performed in a multi-component system containing VO^{2+}, Fe^{3+}, Mn^{2+}, Co^{2+} and Cu^{2+}. 0.3 g of either *U-CMC-SAL* or *N-CMC-SAL* microspheres resin were immersed in 300 mL solution containing a mixture of the previously mentioned metal ions each with initial concentration of 20 mg/L at pH 5, 30 °C and 150 rpm for 3 h. After the adsorption process was accomplished, the residual content of each metal ion component was estimated using atomic absorption.

Table 1
Elemental analysis of modified and unmodified CMC samples.

Sample	C (%)	H (%)	N (%)
CMC	40.3	5.8	0.03
Al-CMC	39.1	5.7	0.026
CMC-g-PAN	55.9	4.6	15.6
CMC-g-PAH	41.4	7.4	34.4
CMC-SAL	59.3	5.5	19.5
U-CMC-SAL	63.2	6.3	17.8

The selectivity coefficient can be anticipated using the following equation (Zhou, Shang, Liu, Huang, & Adesina, 2012)

$$B_{UO_2^{2+}/M^{n+}} = \frac{D_{UO_2^{2+}}}{D_{M^{n+}}} \tag{4}$$

where $D_{UO_2^{2+}}$ and $D_{M^{n+}}$ can be defined as the distribution coefficient of the UO_2^{2+} ions and the other metal ion present in the system, respectively. Also, the distribution coefficient (D) can be estimated by applying the following expression:

$$D = \frac{[(C_i - C_e)/C_e]V}{W} \tag{5}$$

Finally, the ion imprinting effect on the selectivity of the prepared surface ion imprinted microspheres resin was measured by calculation of the relative selectivity coefficient β_r, by applying the following equation (Monier & Abdel-Latif, 2013b)

$$\beta_r = \frac{\beta_{\text{imprint}}}{\beta_{\text{non-imprint}}} \tag{6}$$

where β_{imprint} and $\beta_{\text{non-imprint}}$ are the selectivity coefficients of *U-CMC-SAL* and *N-CMC-SAL* microspheres resin, respectively.

2.6.6. Desorption and reusability experiments

0.5 M HNO_3 solution was utilized for desorption and regeneration of the microspheres. The UO_2^{2+} loaded microspheres were rinsed with distilled water to remove the non-adsorbed metal ion. The resin was then soaked in 100 mL 0.5 M HNO_3 as a desorbing solution. The mixture was agitated for 4 h at 30 °C using mechanical stirrer at 150 rpm. The concentration of the released UO_2^{2+} was calculated and the microspheres resin were extracted and reused in five consecutive adsorption–desorption cycles.

3. Results and discussion

3.1. Characterization of the microspheres samples

A fast evaluation test using $FeCl_3$ was utilized to confirm the presence of the salicylaldehyde hydrazone onto the resin microspheres. The chelating *CMC-SAL* microspheres resin exhibited a deep violet color after treatment with $FeCl_3$ solution which could be attributed to the widely common interaction between the phenolic —OH group and the Fe^{3+} ions.

The elemental analysis of pure CMC, Al-cross-linked CMC microspheres, CMC-g-PAN, CMC-g-PAH, CMC-SAL and U-CMC-SAL were investigated and the results are summarized in Table 1. As can be noticed, the increasing trends in nitrogen and carbon contents provide an evidence for the grafting and subsequent modification by salicylaldehyde insertion onto the grafted chain.

The FTIR spectra were employed to detect the consecutive modification steps of the CMC and the results were presented in Fig. 1. As can be seen, the spectrum of the pure unmodified CMC (Fig. 1a) exhibited a broad distinctive peak at around 3200 cm^{-1} which attributed to the O—H stretching vibrations in addition to a sharp peak at about 1620 cm^{-1} corresponding to the carbonyl group. Furthermore, the spectrum of the CMC-g-PAN (Fig. 1b) confirms the

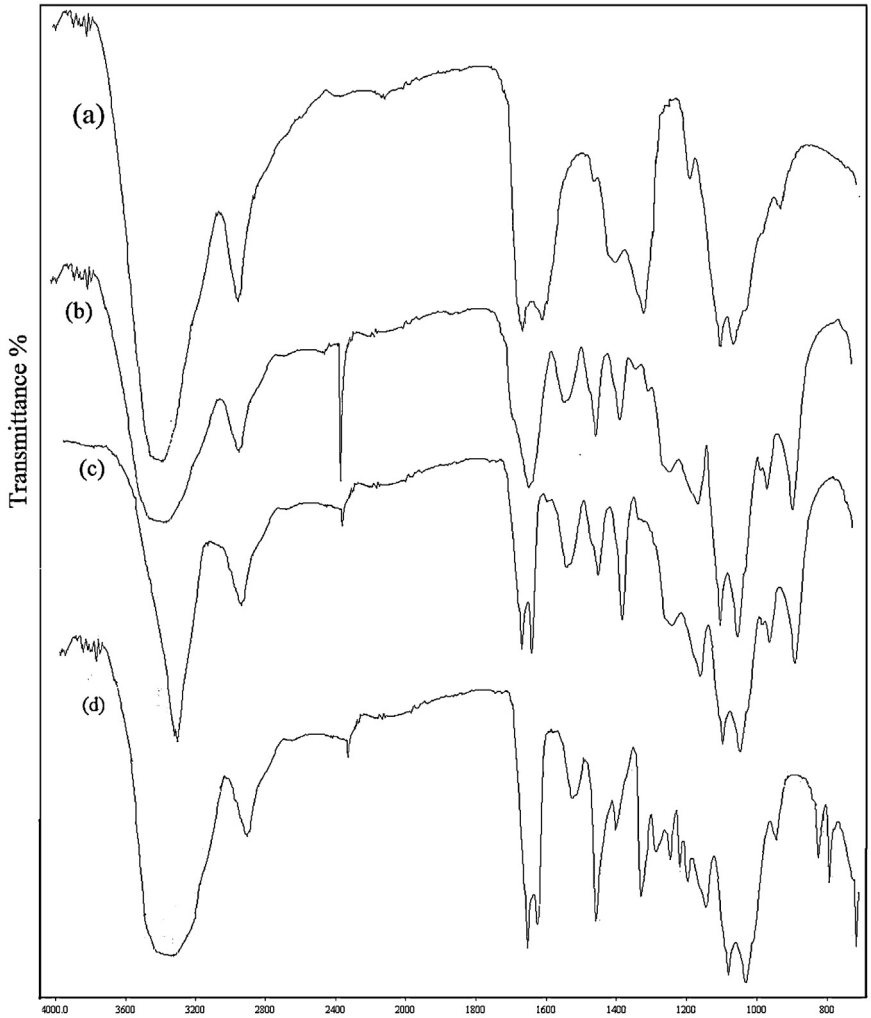

Fig. 1. FTIR spectra of (a) native CMC, (b) CMC-g-PAN, (c) CMC-g-PAH and (d) CMC-SAL.

insertion of the grafted PAN chains onto the CMC backbone by the presents of a new peak at 2370 cm^{-1} which is characteristic for the cyano groups. In addition, the further modification by turning the vast majority of the grafted —CN groups into HN=C—NH—NH_2 was clarified in the spectrum of CMC-g-PAH (Fig. 1c) through the clear disappearance of the characteristic —CN sharp peak at 2370 cm^{-1} and appearance of a new peak at about 1640 cm^{-1} which could be attributed to the newly formed C=N bond. Also, the spectrum of the CMC-SAL (Fig. 1d) gives an evidence for the functionalization with salicylaldehyde moieties by the obvious increase of the peak intensity at 1640 cm^{-1} as a result of the formation of the hydrazone C=N bond in addition to the bands at 1580, 1280, and 750 cm^{-1} which are attributed to the C=C, C—O, and C—H stretching in the aromatic ring, respectively (Guinesi & Cavalheiro, 2006; Monier, Ayad, Wei, & Sarhan, 2010).

For anticipation of the grafting and modification effects on the crystallinity, wide angle X-ray diffraction spectra were utilized to examine the crystallinity degree of the prepared CMC microspheres prior to each modification step and the results were introduced in Fig. 2. As can be noticed the crystallinity pattern of the native CMC exhibited a characteristic peak at $2\theta = 22.5^{\circ}$ (Fig. 2a) correspond to a diffraction plane (1 1 0), which provide a proof for the polysaccharide semi-crystalline structure (Li, Wu, Mu, & Lin, 2011; Zhao et al., 2009). Moreover, the crystallinity profile of CMC-g-PAN (Fig. 2b) presents a sharp crystallinity peak at about $2\theta = 17^{\circ}$ belonging to overlapped diffraction planes of (1 1 0) and (2 0 0) corresponding

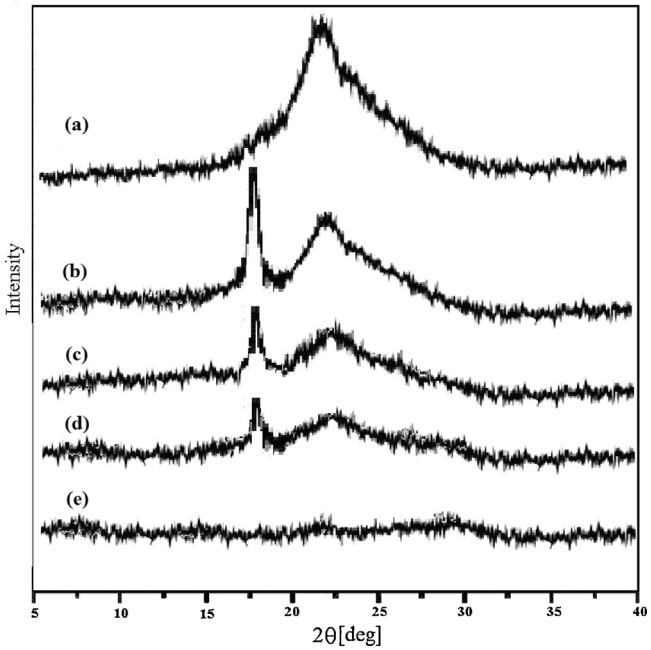

Fig. 2. X-ray diffraction pattern of of (a) native CMC, (b) CMC-g-PAN, (c) CMC-g-PAH and (d) CMC-SAL, (e) formaldehyde cross-linked CMC-SAL.

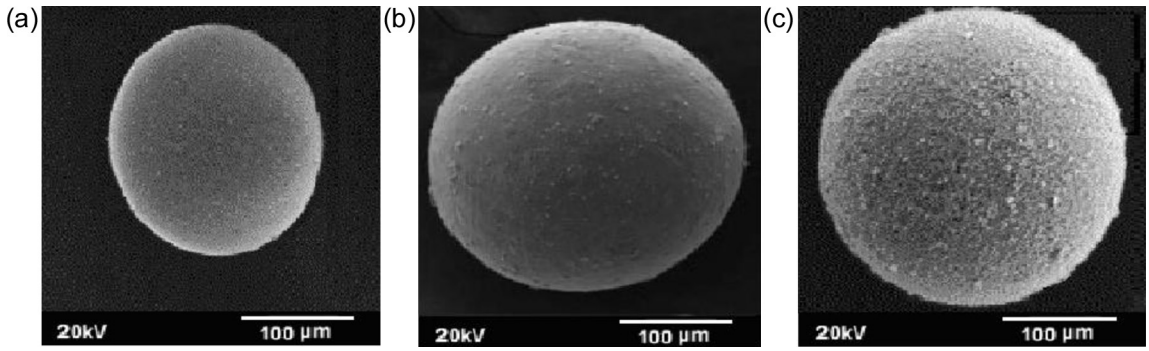

Fig. 3. SEM photos of modified and unmodified CMC microspheres. (a) Cross-linked unmodified CMC microspheres, (b) N-CMC-SAL, and (c) U-CMC-SAL.

to long PAN chains crystal plane (Sarhan, Monier, Ayad, & Badawy, 2010). However, the intensity of the aforementioned crystallinity peak of the CMC at $2\theta = 17^\circ$ was clearly lowered, which indicate the decrease of the crystallinity of the main polysaccharide backbone upon grafting. Furthermore, the further modification of the grafted microspheres through conversion of the —CN into HN=C—$NHNH_2$ followed by salicylaldehyde hydrazone formation (Fig. 2c and d) had greatly lowered the crystallinity of the grafted chains. Upon the formaldehyde cross-linking, the microspheres exhibited an amorphous structure pattern (Fig. 2e) as a consequence of the hydrogen bond cleavage and formation of a cross-linked network.

The surface morphologies of the cross-linked CMC, ion-imprinted U-CMC-SAL and non-imprinted N-CMC-SAL were visualized using scanning electron microscope and the photos are presented in Fig. 3. When compared to the CMC microspheres, both U-CMC-SAL and N-CMC-SAL exhibited a clear diameter increase, which could be attributed to the insertion of the grafted modified chains onto the CMC microspheres. Moreover, the ion imprinted U-CMC-SAL showed an obvious rough and porous surface when compared to the non-imprinted N-CMC-SAL which may be due to the removal of the template UO_2^{2+} from the cross-linked network generated on the microspheres surface. These results were in accordance with that obtained from the BET surface areas measurements, both N-CMC-SAL and U-CMC-SAL presenting surface areas of 45.5 and 167.8 m^2/g, respectively

3.2. UO_2^{2+} adsorption experiments

3.2.1. Influence of pH

Generally, the metal ion removal is greatly influenced by the initial pH of the medium (Zhou et al., 2012). In this study, the removal of UO_2^{2+} by both U-CMC-SAL and N-CMC-SAL was examined as a function of the pH of the adsorption solution system and the results were shown in Fig. 4. As can be observed, in both cases, the UO_2^{2+} ions removal was greatly enhanced by raising the pH and the optimum pH for the adsorption process was estimated to be 5. The maximum percent removal of the ion-imprinted U-CMC-SAL and non-imprinted N-CMC-SAL toward UO_2^{2+} were estimated to be 97% and 55% respectively, which may confirm the effect of the imprinting on the selectivity of the prepared microspheres resin. Under stronger acidic conditions, at lower pH values, the percent removal of UO_2^{2+} onto both U-CMC-SAL and N-CMC-SAL microspheres exhibited a significant decrease, which could be explained as a result of the electrostatic repulsion forces due to the protonation of the active sites to which the metal ions will coordinate (Bingjie, Dongfeng, Haiyan, Ying, & Li, 2011).

The removal of the UO_2^{2+} at almost neutral or slightly acidic pH values may give an evidence for the adsorption through the coordination between the active chelating sites which was inserted onto the microspheres resin and the UO_2^{2+} cation which was clearly presented in Scheme 2 and previously reported (Sessler, Melfi, & Pantos, 2006). The H^+ release upon the complex formation was confirmed by the obvious pH lowering to about 3.5 after the adsorption process.

3.2.2. Thermodynamics of adsorption

In order to evaluate the thermodynamic parameters of UO_2^{2+} adsorption onto both ion-imprinted U-CMC-SAL and non-imprinted N-CMC-SAL microspheres resin, the adsorption experiment was carried out in a system contain 0.03 g of the microspheres resin under study, 30 mL of 30 mg/L UO_2^{2+} solution in a range of temperature changed from 293 to 313 K. For both studied systems, the amounts of UO_2^{2+} adsorbed were decreased gradually as the temperature increases, which may indicate the exothermic nature of the adsorption process. For more details regarding the adsorption equilibrium, the thermodynamic parameters including the entropy (ΔS°), enthalpy (ΔH°) and Gibbs free energy (ΔG°) were estimated using the following series of equations (Lulu, Chuannan, Zhen, Fuguang, & Huamin, 2011; Monier & Abdel-Latif, 2012).

$$K_C = \frac{C_{ad}}{C_e} \tag{7}$$

where C_{ad} is the amount of the adsorbed UO_2^{2+} ions onto the microspheres resin at equilibrium (mg/g) and C_e is concentration of the UO_2^{2+} ions in the solution at equilibrium (mg/L).

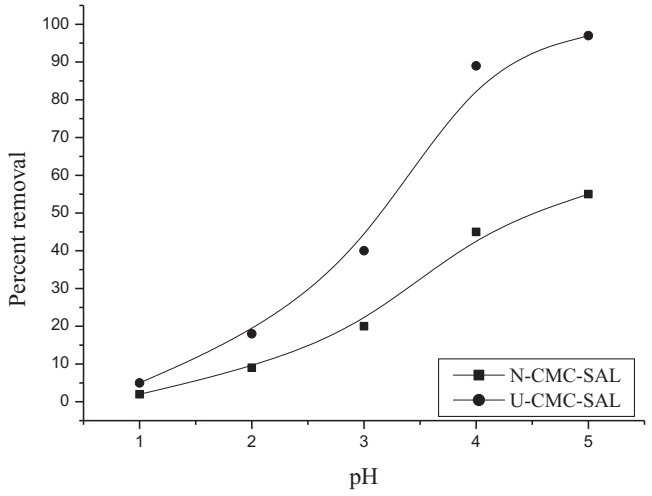

Fig. 4. Effect of pH on the uptake of UO_2^{2+} ions by U-CMC-SAL and N-CMC-SAL (initial concentration 100 mg/L; adsorbent. 1 g/L; contact time 3 h; shaking rate 150 rpm, 30 °C).

Table 2
Thermodynamic parameters for the uptake of UO_2^{2+} on U-CMC-SAL and N-CMC-SAL resin.

System	K_C			$-\Delta G^\circ_{ads}$ (kJ/mol)			ΔH°_{ads} (kJ/mol)	ΔS°_{ads} (J/mol K)
	293 K	303 K	313 K	293 K	303 K	313 K		
U-CMC-SAL	149.02	36.50	24.01	12.11	9.08	8.27	−70.52	−200.02
N-CMC-SAL	32.30	19.13	14.00	8.46	7.42	6.87	−32.19	−81.16

The Gibbs free energy of adsorption (ΔG°_{ads}) using the following equation:

$$\Delta G^\circ_{ads} = -RT \ln K_C \quad (8)$$

Also, the anticipation of both enthalpy (ΔH°_{ads}) and entropy (ΔS°_{ads}) of adsorption were achieved by plotting $\ln K_C$ against $1/T$ (Fig. 5) in accordance with the following equation:

$$\ln K_C = \frac{\Delta S^\circ_{ads}}{R} - \frac{\Delta H^\circ_{ads}}{RT} \quad (9)$$

where R (8.314 J/mol K) is the gas constant.

The results from the above calculations were summarized in Table 2 and as can be observed, the ΔG°_{ads} negative values for both ion-imprinted U-CMC-SAL and non-imprinted N-CMC-SAL microspheres resin confirms that the adsorption process is a spontaneous process. In addition, the exothermic nature of the adsorption process was obviously confirmed from the estimated negative values of the ΔH°_{ads}. Also, the entropy changes (ΔS°_{ads}) during the adsorption process exhibited negative results in all studied system which could be explained as a result of the aggregation of the reacting UO_2^{2+} species onto the microspheres adsorbent resin which needless to say will decrease the randomness of the system and subsequently lower the entropy. These results were in accordance with previous results by Zhou et al. (2012) where UO_2^{2+} was selectively adsorbed using ion-imprinted magnetic chitosan resin and Monier & Abdel-Latif (2013b) where Hg^{2+} was selectively adsorbed using surface ion-imprinted modified PET fibers.

3.2.3. Kinetics of UO_2^{2+} adsorption

For achieving a suitable design for the adsorption system, the adsorption kinetics should be examined in order to provide further details regarding the rate and mechanism of the studied adsorption process (Lesmana, Febriana, Soetaredjo, Sunarso, & Ismadji, 2009). Fig. 6 exhibits the variation of the adsorbed amounts of UO_2^{2+} by both ion-imprinted U-CMC-SAL and non-imprinted N-CMC-SAL microspheres resin as a function of the adsorption time. As can be noticed in both cases the adsorption was fast during the initial adsorption period with initial rate of 2.62 and 1.73 mg/g min^{-1} for U-CMC-SAL and N-CMC-SAL respectively, and then reach equilibrium in about 100 min. The observed initial rapid UO_2^{2+} uptake particularly with U-CMC-SAL could be attributed to the higher availability of the active chelating sites on the microspheres resin adsorbent which gradually reduced as the adsorption process continued to the equilibrium. In addition, the higher adsorption of the UO_2^{2+} by U-CMC-SAL compared to N-CMC-SAL could be explained due to the higher surface area and higher affinity of the ion-imprinted microspheres to the UO_2^{2+} ions which results from the geometric shape, size and chemical functionality matching of the active recognition complexing sited created after removal of the template ions from the cross-linked polymeric network (Zhou et al., 2012).

In order to evaluate the mechanism of the adsorption, the obtained kinetic data were employed to fit with the well known pseudo-first order, Eq. (10) and pseudo-second order, Eq. (11) kinetic models (Bingjie et al., 2011; Zhou et al., 2012).

$$\frac{1}{q_t} = \frac{k_1}{q_{e1} t} + \frac{1}{q_e} \quad (10)$$

$$\frac{t}{q_t} = \frac{1}{k_2 q_{e2}^2} + \left(\frac{1}{q_e}\right) t \quad (11)$$

where q_e and q_t (mg/g) are the adsorbed amounts of UO_2^{2+} ions at equilibrium and at time (t), respectively, k_1 (min^{-1}) and k_2 (g mg^{-1} min^{-1}) refer to the rate constants of both pseudo-first order and pseudo-second order, respectively. The pseudo-first order parameters q_{e1} and k_1 can be calculated by plotting the reciprocal of q_t against the reciprocal of (t). Also, the pseudo-second order parameters q_{e2} and k_2 were calculated by plotting t/q_t against (t). The kinetic parameters estimated from the aforementioned models were summarized in Table 3. As can be seen, the correlation coefficients, R^2, obtained from the second order equation exhibited a greater values compared to that of the first order equation.

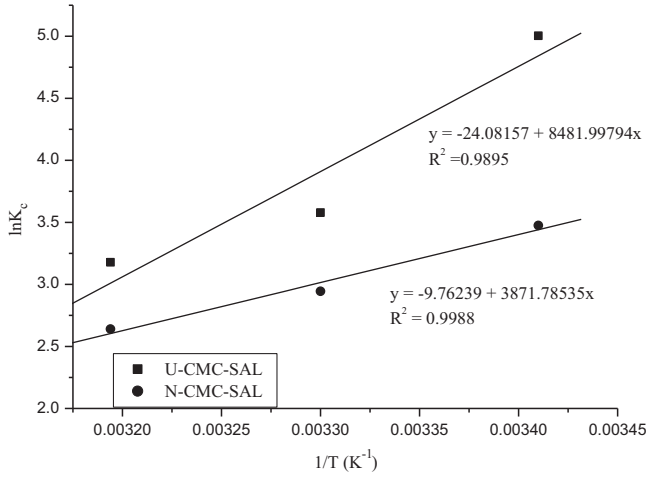

Fig. 5. Plot of $\ln K_C$ as a function of reciprocal of temperature ($1/T$) for the adsorption of UO_2^{2+} by U-CMC-SAL and N-CMC-SAL resins.

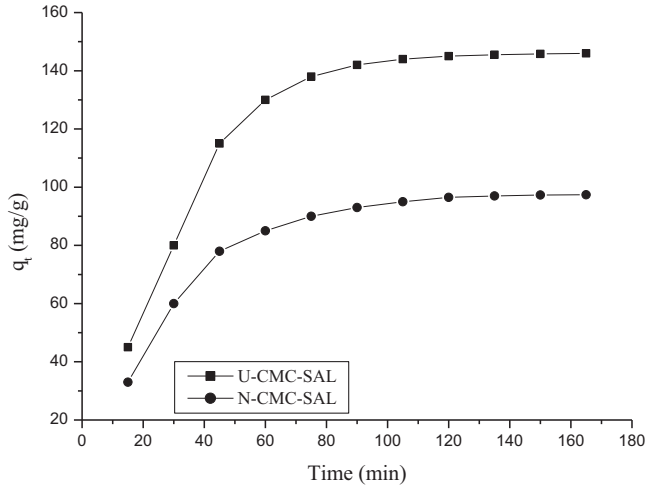

Fig. 6. Effect of contact time on the uptake of UO_2^{2+} ions by U-CMC-SAL and N-CMC-SAL resins (initial concentration 150 mg/L, adsorbent 1 g/L, pH 5.0, shaking rate 150 rpm, 30 °C).

Table 3
Kinetic parameters for UO_2^{2+} uptake by U-CMC-SAL and N-CMC-SAL resin.

Adsorbent	First-order model		R^2
	k_1 (min^{-1})	q_{e1} (mg/g)	
U-CMC-SAL	38.765	144 ± 4	0.9234
N-CMC-SAL	31.120	93 ± 3	0.9154
Adsorbent	Second-order model		R^2
	k_2 (g mg^{-1} min^{-1})	q_{e2} (mg/g)	
U-CMC-SAL	2.65×10^{-4}	148 ± 0.5	0.9998
N-CMC-SAL	4.82×10^{-4}	95 ± 1	0.9987

Moreover the adsorbed UO_2^{2+} amounts estimated from the second-order model closer to the experimental values when compared to that obtained from the first-order model. These findings indicate that the kinetic data of the studied adsorption system fit better with the second-order kinetic model, which may give evidence that the chelation and complexation involving the share of electrons between the active sites of the microspheres adsorbent and the UO_2^{2+} ions is the rate limiting step. As shown in Scheme 2 the UO_2^{2+} ions can form stable six-membered ring with the salicylaldehyde hydrazone moieties introduced onto the modified CMC microspheres resin this (Sessler et al., 2006).

In many of previous work (Monier & Abdel-Latif, 2013a) where Hg^{2+} was selectively separated by surface ion-imprinted fibers based on PET (Zhou et al., 2012) where UO_2^{2+} ions were selectively adsorbed onto ion-imprinted magnetic chitosan resin (Lulu et al., 2011) in which Ag^+ was removed using modified thiourea-chitosan magnetic resin and (Bingjie et al., 2011) where modified ion imprinted magnetic chitosan was utilized for removal of As(III), the adsorption kinetics followed the second order model which is in accordance with the results in our current study.

3.2.4. Evaluation of the adsorption isotherms

The basic physic-chemical behavior provided by examining the adsorption isotherms, makes it essential during the studying of the adsorption process (Bingjie et al., 2011). For this purpose, a variety of UO_2^{2+} initial concentrations ranged from 10 to 400 mg/L were employed and the adsorption isotherms for both U-CMC-SAL and N-CMC-SAL are shown in Fig. 7.

In order to analyze the obtained results, both Langmuir and Freundlich models were utilized. The Langmuir model, which

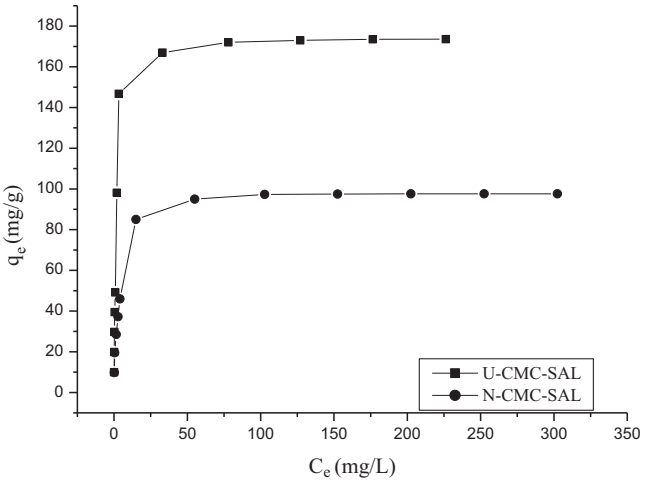

Fig. 7. Adsorption isotherms of UO_2^{2+} ions by U-CMC-SAL and N-CMC-SAL resins (initial concentration 10–400 mg/L, adsorbent 1 g/L, pH 5.0, shaking rate 150 rpm, 30 °C).

Table 4
Parameters for UO_2^{2+} ions adsorption by U-CMC-SAL and N-CMC-SAL resin according to different equilibrium models.

Adsorbent	Langmuir isotherm constants		R^2
	K_L (L/g)	q_m (mg/g)	
U-CMC-SAL	76.2×10^{-2}	180 ± 1	0.9998
N-CMC-SAL	2.716	97 ± 1	0.9999
Adsorbent	Freundlich isotherm constants		R^2
	K_F	n	
U-CMC-SAL	45.904	3.219	0.9121
N-CMC-SAL	24.477	3.492	0.9237

assumed that the adsorption takes place on homogeneous surface, the adsorbate forms a monolayer on the adsorbent by accommodation on energetically equivalent sites and there is no interactions between the adsorbate molecules can be mathematically represented by the following equation:

$$\frac{C_e}{q_e} = \left(\frac{1}{K_L q_m}\right) + \left(\frac{C_e}{q_m}\right) \quad (12)$$

where q_e is the equilibrium adsorption capacity (mg/g), C_e is the equilibrium concentration of the UO_2^{2+} (mg/L), respectively, q_m is the maximum adsorption capacity of UO_2^{2+} (mg/g) and K_L is the Langmuir constant (L/mg) which correspond to the adsorption energy and binding sites affinity.

Furthermore, the empirical Freundlich isotherm model, which describes the multilayer adsorption on energetically heterogeneous sites can be mathematically expressed by the following equations:

$$\ln q_e = \ln K_F + \frac{1}{n} \ln C_e \quad (13)$$

where K_F and n are empirical constants those indicate the relative sorption capacity and sorption intensity, respectively.

The results obtained from the fit of the data within the aforementioned mathematical models were collected in Table 4. As can be seen, the results shows that Langmuir isotherm model is the best model for describing the adsorption process with R^2 values >0.999 which give an evidence for the homogeneous monolayer formation. In addition, the ion imprinted U-CMC-SAL exhibited a significant maximum adsorption capacity of 180 ± 1 mg/g compared to the non-imprinted N-CMC-SAL (97 ± 1 mg/g) which could be explained as a result of the imprinting effect in addition to the higher surface area formed due to the porous morphological structure as shown in Fig. 3.

The adsorption possibility can be evaluated by calculation of the separation factor constant (R_L) according to the following equation (Monier & Abdel-Latif, 2013a):

$$R_L = \frac{1}{1 + C_0 K_L} \quad (14)$$

where K_L is the Langmuir constant and C_0 (10–400 mg/L) is the initial UO_2^{2+} concentration. $R_L > 1.0$, unsuitable; $R_L = 1$, linear; $0 < R_L < 1$, suitable; $R_L = 0$, irreversible. The estimated R_L values for ion-imprinted U-CMC-SAL resin ranged between 0.00327 and 0.116 which confirm the validity of the imprinted resin for UO_2^{2+} uptake.

In many previous works, various adsorbents were developed for UO_2^{2+} uptake, *i.e.* ion-imprinted magnetic chitosan resin (Zhou et al., 2012), which exhibited a maximum adsorption capacity 187 mg/g, ion-imprinted chitosan/PVA cross-linked hydrogel (Liu et al., 2010) in which a maximum adsorption capacity of 156 mg/g was obtained and Merrifield chloromethylated resin anchored with semicarbazone moiety (Jain, Handa, Sait, Shrivastav, & Agrawal, 2001), which present a maximum adsorption capacity 48 mg/g. By

Table 5
Selective adsorption of UO_2^{2+} from multicomponent mixtures by U-CMC-SAL and N-CMC-SAL resin (initial concentration 20 mg/L, adsorbent 1 g/L, shaking rate 150 rpm, solution pH 5.0, 30 °C).

	Distribution ratio (L/g)		Selectivity coefficient, $\beta_{UO_2^{2+}/M^{n+}}$		Relative selectivity coefficient, β_r
Metal	U-CMC-SAL	N-CMC-SAL	U-CMC-SAL	N-CMC-SAL	
UO_2^{2+}	221.22	35.36	–	–	
VO^{2+}	4.4	3.88	50.27	9.11	5.52
Fe^{3+}	6.41	65.67	34.51	0.54	25.69
Mn^{2+}	2.68	2.23	21.55	15.86	63.9
Co^{2+}	2.81	3.17	82.54	11.15	7.40
Cu^{2+}	5.25	5.89	42.14	6	7.02

comparison, the prepared ion-imprinted microspheres resin exhibited a good capacity for adsorption of UO_2^{2+} ions.

3.2.5. Evaluation of the selective uptake of UO_2^{2+}

In order to anticipate the selectivity of the prepared ion-imprinted microspheres resin toward UO_2^{2+} ions, the distribution ratios and selectivity coefficients related to other metal cations which may coordinate in a similar manner with UO_2^{2+} were estimated by performing the selective uptake experiments using both U-CMC-SAL and N-CMC-SAL and the results were presented in Table 5. According to the obtained results, the distribution ratio of U-CMC-SAL for UO_2^{2+} ions was more than 6-folds higher when compare to that of N-CMC-SAL. On the other hand, when we compare the relative selectivity coefficient of U-CMC-SAL with respect to each studied metal ion, it was found obviously greater than 1. Based on these results its clear that the prepared ion-imprinted U-CMC-SAL exhibited an obvious selectivity toward the UO_2^{2+} ions compared to the non-imprinted N-CMC-SAL which could be explained as a result of the formation of the recognition sites on the cross-linked network on the surface of the microspheres resin, which match in she shape, size and geometry of the UO_2^{2+} ions.

3.2.6. Microspheres resin regeneration

For the regeneration of the ion-imprinted U-CMC-SAL resin, desorption was carried out using 0.5 M HNO_3 for five consecutive adsorption–desorption cycles and the efficiency was estimated utilizing the following equation (Zhou et al., 2012).

$$\text{Regeneration efficiency (\%)} = \left(\frac{UO_2^{2+} \text{ absorben in the 2nd time}}{UO_2^{2+} \text{ absorben in the 1st time}}\right) \times 100 \quad (15)$$

After the fifth cycle, the microspheres resin maintains about 92% of its original efficiency. In addition, the resin exhibited less than 1% loss from its original weight.

4. Conclusion

Herein, the surface ion-imprinting technique was utilized for the manufacturing of surface ion-imprinted chelating microspheres resin based on modified salicylaldehyde-carboxymethyl cellulose (U-CMC-SAL) in presence of UO_2^{2+} ions as an imprint ion and formaldehyde as a cross-linker. Different instrumental techniques such as elemental analysis, scanning electron microscope (SEM), FTIR and X-ray diffraction spectra were employed for full characterization of the prepared polymeric samples. The prepared resin exhibited a higher capability for selective adsorption of UO_2^{2+} when compared to the non-imprinted resin (N-CMC-SAL). Also, different important parameters such as pH, temperature, time and initial metal ion concentration were investigated in order to evaluate the optimum condition for the adsorption process. The results indicated that pH 5 was the best for the UO_2^{2+} uptake, in addition, the adsorption was exothermic in nature, follows the second-order kinetics and the adsorption isotherm showed the best fit with Langmuir isotherm model with maximum adsorption capacity of 180 ± 1 and 97 ± 1 mg/g for both U-CMC-SAL and N-CMC-SAL respectively. Desorption and regeneration were carried out using 0.5 M HNO_3 solution and the results confirmed that the resin keeps about 92% of its original efficiency after five consecutive adsorption–desorption operations.

References

Abdel-Halim, E. S., & Al-Deya, S. S. (2012). Chemically modified cellulosic adsorbent for divalent cations removal from aqueous solutions. *Carbohydrate Polymers*, *87*, 1863–1868.

Aghaei, A., Hosseini, M. R. M., & Najafi, M. (2010). A novel capacitive biosensor for cholesterol assay that uses an electropolymerized molecularly imprinted polymer. *Electrochimica Acta*, *55*, 1503–1508.

Andersson, L. I. (1996). Application of molecular imprinting to the development of aqueous buffer and organic solvent based radioligand binding assays for (*S*)-propranolol. *Analytical Chemistry*, *68*, 111–117.

Bajpai, A. K., & Giri, A. (2003). Water sorption behaviour of highly swelling (carboxy methylcellulose-g-polyacrylamide) hydrogels and release of potassium nitrate as agrochemical. *Carbohydrate Polymers*, *53*, 271–279.

Bingjie, L., Dongfeng, W., Haiyan, L., Ying, X., & Li, Z. (2011). As(III) removal from aqueous solution using α-Fe_2O_3 impregnated chitosan beads with As(III) as imprinted ions. *Desalination*, *272*, 286–292.

Guinesi, L. S., & Cavalheiro, E. T. G. (2006). Influence of some reactional parameters on the substitution degree of biopolymeric Schiff bases prepared from chitosan and salicylaldehyde. *Carbohydrate Polymer*, *65*, 557–561.

Haginaka, J. (2009). Molecularly imprinted polymers as affinity-based separation media for sample preparation. *Journal of Separation Science*, *32*, 1548–1565.

Jain, V. K., Handa, A., Sait, S. S., Shrivastav, P., & Agrawal, Y. K. (2001). Preconcentration, separation and trace determination of lanthanum(III), cerium(III), thorium(IV) and uranium(VI) on polymer supported *o*-vanillinsemicarbazone. *Analytica Chimica Acta*, *429*, 237–246.

Jiang, M., Shi, Y., Zhang, R. L., Shi, C. H., Peng, Y., Huang, Z., et al. (2009). Selective molecularly imprinted stationary phases for bisphenol A analysis prepared by modified precipitation polymerization. *Journal of Separation Science*, *32*, 326–3273.

Lesmana, S. O., Febriana, N., Soetaredjo, F. E., Sunarso, J., & Ismadji, S. (2009). Studies on potential applications of biomass for the separation of heavy metals from water and wastewater. *Biochemical Engineering Journal*, *44*, 19–41.

Li, H., Wu, B., Mu, C., & Lin, W. (2011). Concomitant degradation in periodate oxidation of carboxymethyl cellulose. *Carbohydrate Polymers*, *84*, 881–886.

Liu, L. S., & Berg, R. A. (2002). Adhesion barriers of carboxymethylcellulose and polyethylene oxide composite gels. *Journal of Biomedical Material Researches*, *63*, 326–332.

Liu, Y., Cao, X., Hua, R., Wang, Y., Liu, Y., Pang, C., et al. (2010). Selective adsorption of uranyl ion on ion-imprinted chitosan/PVA cross-linked hydrogel. *Hydrometallurgy*, *104*, 150–155.

Lulu, F., Chuannan, L., Zhen, L., Fuguang, L., & Huamin, Q. (2011). Removal of Ag^+ from water environment using a novel magnetic thiourea-chitosan imprinted Ag^+. *Journal of Hazardous Materials*, *194*, 193–201.

Mayes, A. G., & Mosbach, K. (1996). Molecularly imprinted polymer beads: Suspension polymerization using a liquid perfluorocarbon as the dispersing phase. *Analytical Chemistry*, *68*, 3769–3774.

Mocanu, G., Mihai, D., LeCerf, D., Picton, L., & Muller, G. (2004). Synthesis of new associative gel microspheres from carboxymethyl pullulan and their interactions with lysozyme. *European Polymer Journal*, *40*, 283–289.

Mohy Eldin, M. S., El-Sherif, H. M., Soliman, E. A., Elzatahry, A. A., & Omer, A. M. (2011). Polyacrylamide-grafted carboxymethyl cellulose: Smart pH-sensitive hydrogel for protein concentration. *Journal of Applied Polymer Science*, *122*, 469–479.

Monier, M., & Abdel-Latif, D. A. (2012). Preparation of cross-linked magnetic chitosan-phenylthiourea resin for adsorption of Hg(II), Cd(II) and Zn(II) ions from aqueous solutions. *Journal of Hazardous Materials*, *209–210*, 240–249.

Monier, M., & Abdel-Latif, D. A. (2013a). Modification and characterization of PET fibers for fast removal of Hg(II), Cu(II) and Co(II) metal ions from aqueous solutions. *Journal of Hazardous Materials*, *250/251*, 122–130.

Monier, M., & Abdel-Latif, D. A. (2013b). Synthesis and characterization of ion-imprinted chelating fibers based on PET for selective removal of Hg^{2+}. *Chemical Engineering Journal*, *221*, 452–460.

Monier, M., Ayad, D. M., Wei, Y., & Sarhan, A. A. (2010). Adsorption of Cu(II), Co(II), and Ni(II) ions by modified magnetic chitosan chelating resin. *Journal of Hazardous Materials*, *177*, 962–970.

Ozcan, L., & Sahin, Y. (2007). Determination of paracetamol based on electropolymerized-molecularly imprinted polypyrrole modified pencil graphite electrode. *Sensors and Actuators B*, *127*, 362–369.

Pasetto, P., Maddock, S. C., & Resmini, M. (2005). Synthesis and characterisation of molecularly imprinted catalytic microgels for carbonate hydrolysis. *Analytica Chimica Acta*, *542*, 66–75.

Perez, N., Whitcombe, M. J., & Vulfson, E. N. (2000). Molecularly imprinted nanoparticles prepared by core–shell emulsion polymerization. *Journal of Applied Polymer Science*, *77*, 1851–1859.

Qin, L., He, X.-W., Zhang, W., Li, W.-Y., & Zhang, Y.-K. (2009). Surface-modified polystyrene beads as photografting imprinted polymer matrix for chromatographic separation of proteins. *Journal of Chromatography A*, *1216*, 807–814.

Sambe, H., Hoshina, K., & Haginaka, J. (2007). Molecularly imprinted polymers for triazine herbicides prepared by multi-step swelling and polymerization method: Their application to the determination of methylthiotriazine herbicides in river water. *Journal of Chromatography A*, *1152*, 130–137.

Sand, A., Yadav, M., & Behari, K. (2010). Preparation and characterization of modified sodium carboxymethyl cellulose via free radical graft copolymerization of vinyl sulfonic acid in aqueous media. *Carbohydrate Polymers*, *81*, 97–103.

Sarhan, A. A., Monier, M., Ayad, D. A., & Badawy, D. S. (2010). Evaluation of the potential of polymeric carriers based on chitosan-grafted-polyacrylonitrile in the formulation of drug delivery systems. *Journal of Applied Polymer Science*, *118*, 1837–1845.

Sergeyeva, T. A., Slinchenko, O. A., Gorbach, L. A., Matyushov, V. F., Brovko, O. O., Piletsky, S. A., et al. (2010). Catalytic molecularly imprinted polymer membranes: Development of the biomimetic sensor for phenols detection. *Analytica Chimica Acta*, *659*, 274–279.

Sessler, J. L., Melfi, P. J., & Pantos, G. D. (2006). Uranium complexes of multidentate N-donor ligands. *Coordination Chemistry Reviews*, *250*, 816–843.

Suedee, R., Bodhibukkana, C., Tangthong, N., Amnuaikit, C., Kaewnopparat, S., & Srichana, T. (2008). Development of a reservoir-type transdermal enantioselective-controlled delivery system for racemic propranolol using a molecularly imprinted polymer composite membrane. *Journal of Controlled Release*, *129*, 170–178.

Suedee, R., Jantarat, C., Lindner, W., Viernstein, H., Songkro, S., & Srichana, T. (2010). Development of a pH-responsive drug delivery system for enantioselective-controlled delivery of racemic drugs. *Journal of Controlled Release*, *142*, 122–131.

Tripathy, J., Mishra, D. K., & Behari, K. (2009). Graft copolymerization of N-vinylformamide onto sodium carboxymethylcellulose and study of its swelling, metal ion sorption and flocculation behaviour. *Carbohydrate Polymers*, *75*, 604–611.

Xu, X., Chen, S., & Wu, Q. (2012). Surface molecular imprinting on polypropylene fibers for rhodamine B selective adsorption. *Journal Colloids and Interface Science*, *285*, 193–201.

Xu, P. P., Xu, W. Z., Zhang, X. J., Pan, J. M., & Yan, Y. S. (2010). Molecularly-imprinted material for dibenzothiophene recognition prepared by surface imprinting methods. *Adsorption Science Technology*, *27*, 975–987.

Yao, Q. Z., & Zhou, Y. M. (2009). Surface functional imprinting of bensulfuron-methyl at surface of silica nanoparticles linked by silane coupling agent. *Journal of Inorganic and Organometalic Polymers*, *19*, 215–222.

Ye, L., Cormack, P. A. G., & Mosbach, K. (1999). Molecularly imprinted monodisperse microspheres for competitive radioassay. *Analytical Communication*, *36*, 35–38.

Yin, J. F., Meng, Z. H., Zhu, Y. S., Song, M. Y., & Wang, H. l. (2011). Dummy molecularly imprinted polymer for selective screening of trace bisphenols in river water. *Analytical Methods*, *3*, 173–180.

Zhao, Q., Qian, J. W., An, Q. F., Gui, Z. L., Jin, H. T., & Yin, M. J. (2009). Pervaporation dehydration of isopropanol using homogeneous polyelectrolyte complex membranes of poly(diallyldimethylammonium chloride)/sodium carboxymethyl cellulose. *Journal of Membrane Science*, *329*, 175–182.

Zhou, L., Shang, C., Liu, Z., Huang, G., & Adesina, A. A. (2012). Selective adsorption of uranium(VI) from aqueous solutions using the ion imprinted magnetic chitosan resins. *Journal of Colloid and Interface Science*, *366*, 165–172.

Zhou, H., Xu, Y., Tong, H., Liu, Y., Han, F., Yan, X., et al. (2013). Direct synthesis of surface molecularly imprinted polymers based on vinyl–SiO_2 nanospheres for recognition of bisphenol A. *Journal of Applied Polymer Science*, *128*, 3846–3852.

Zhu, X., Yang, J., Su, Q., Cai, J., & Gao, Y. (2005). Selective solid-phase extraction using molecularly imprinted polymer for the analysis of polar organophosphorus pesticides in water and soil samples. *Journal of Chromatography A*, *1092*, 161–166.